30

Nanowire-Polymer Nanocomposites as Thermal Interface Material

Kafil M. Razeeb[1] and Eric Dalton[2]
[1]*Tyndall National Institute, University College Cork,*
[2]*Stokes Institute, University of Limerick,*
Ireland

1. Introduction

Packaging of semiconductor electronic device is a challenge due to the progressive increase in the power level of operating devices which is associated with the increasing device performance. As semiconductor device feature sizes continue to be reduced, ensuring reliable operation has become a growing challenge. The effective transfer of heat from an integrated circuit (IC) and its heat spreader to a heat sink is a vital step in meeting this challenge. The ITRS projected power density and junction-to-ambient thermal resistance for high-performance chips at the 14 nm generation are >100 Wcm^{-2} and <0.2 $°CW^{-1}$, respectively. The main bottlenecks in reducing the junction-to-ambient thermal resistance are the thermal resistances of the thermal interface material (TIM) (Prasher 2006) and the heat sink. The primary goal of this chapter is to review the metallic-nanowire nanocomposites as thermal interface material compared to other types of thermal interface materials. The first section of the chapter will review different types of nanowire-polymer composites as well as carbon nanotube-polymer composites as thermal interface material. In recent years, carbon nanotube (CNT) and nanotube-polymer composites were proposed in many publications as a possible TIM with high thermal conductivity and low thermal impedance. However, the possibility of inadvertently incorporating contaminating impurities, the existence of voids between CNTs, and the growth conditions of CNT arrays greatly affect the effective thermal conductivity of CNTs, typically resulting in a TIM with a large performance uncertainty. On the other hand, nanowire-polymer nanocomposites can be proposed as thermal interface material where due to the inclusion of nanowires, composites should achieve high thermal conductivity. The later sections of this chapter will describe the research and development ongoing in the area of nanowire-polymer nanocomposites. The fabrication routes for the nanowires and the nanowire-polymer composites as well as the characterizations of the nanocomposites will be discussed in detail. The applicability of metallic nanowire-polymer nanocomposites as thermal interface material will be evaluated.

2. Thermal interface materials

When two nominally flat and smooth solid surfaces are joining together to form a dry joint (Xu 2006) as can be seen in Fig. 1(a), roughnesses on both surfaces limit the actual area of

contact between the two solids to a small percentage (about 1%-2%) of the apparent contact area (Greenwood and Williamson 1966). Therefore, the heat flux through this interface - if neglecting the heat transfer by radiation between the surfaces - flows by two different heat conduction paths: firstly, solid-to-solid conduction through the contact points and secondly, conduction through the air (a poor thermal conductor compared to the solid materials) trapped between the area of non-contact. Those two different heat transfer paths constrict the heat in a confined area: this limiting factor has been called thermal contact impedance. In order to diminish the thermal contact impedance and consequently increase the heat transfer rate, the air gap formed by the mating surfaces must be replaced by a material with a higher thermal conductivity than that of the air: those materials are commonly called TIMs. From Fig. 1(b), the total thermal impedance due to the TIM insertion (θ_{TIM}) between the two mating surfaces can be retrieved as follows (Prasher 2001):

$$\theta_{\mathrm{TIM}} = \frac{\mathrm{BLT}}{\mathrm{k_{TIM}}} + \theta_{c1} + \theta_{c2} \tag{1}$$

where θ_{c1} and θ_{c2} represent the contact impedances of the TIM with the two bounding surfaces, k_{TIM} is the thermal conductivity of the TIM and BLT is its bond line thickness. Since the main objective of thermal management in electronic packaging is the efficient removal of heat from the semiconducting device to the ambient, the total thermal impedance from the junction-to-ambient (θja) *has* to be minimized: the lower the thermal impedance, the lower the temperature drop from the silicon die to the ambient.

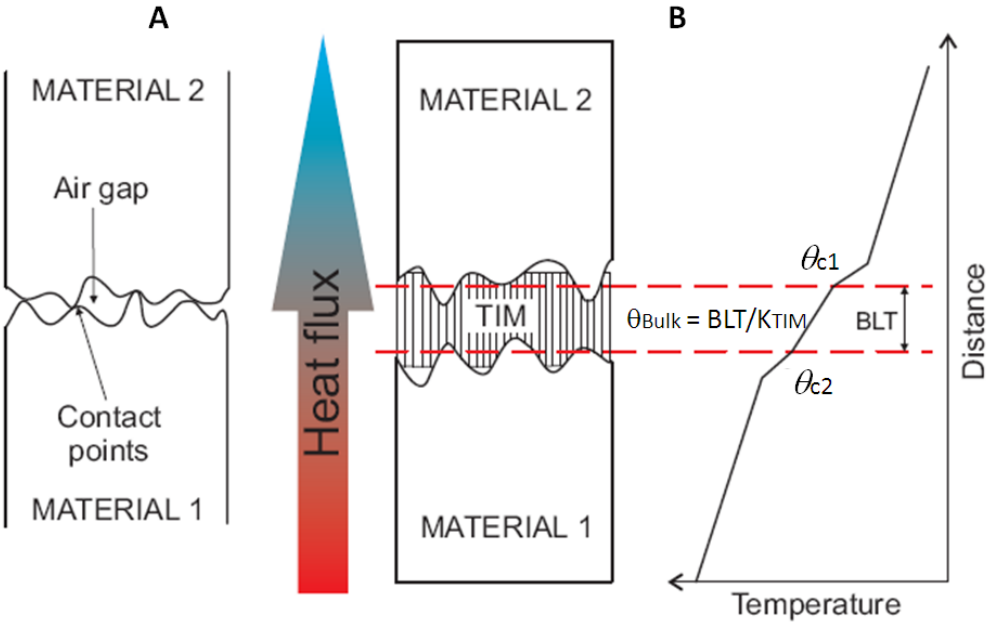

Fig. 1. Sketch showing the real area of contact of a joint formed by two rough surfaces (a); sketch representing a TIM in the real application scenario (b) (Prasher 2006).

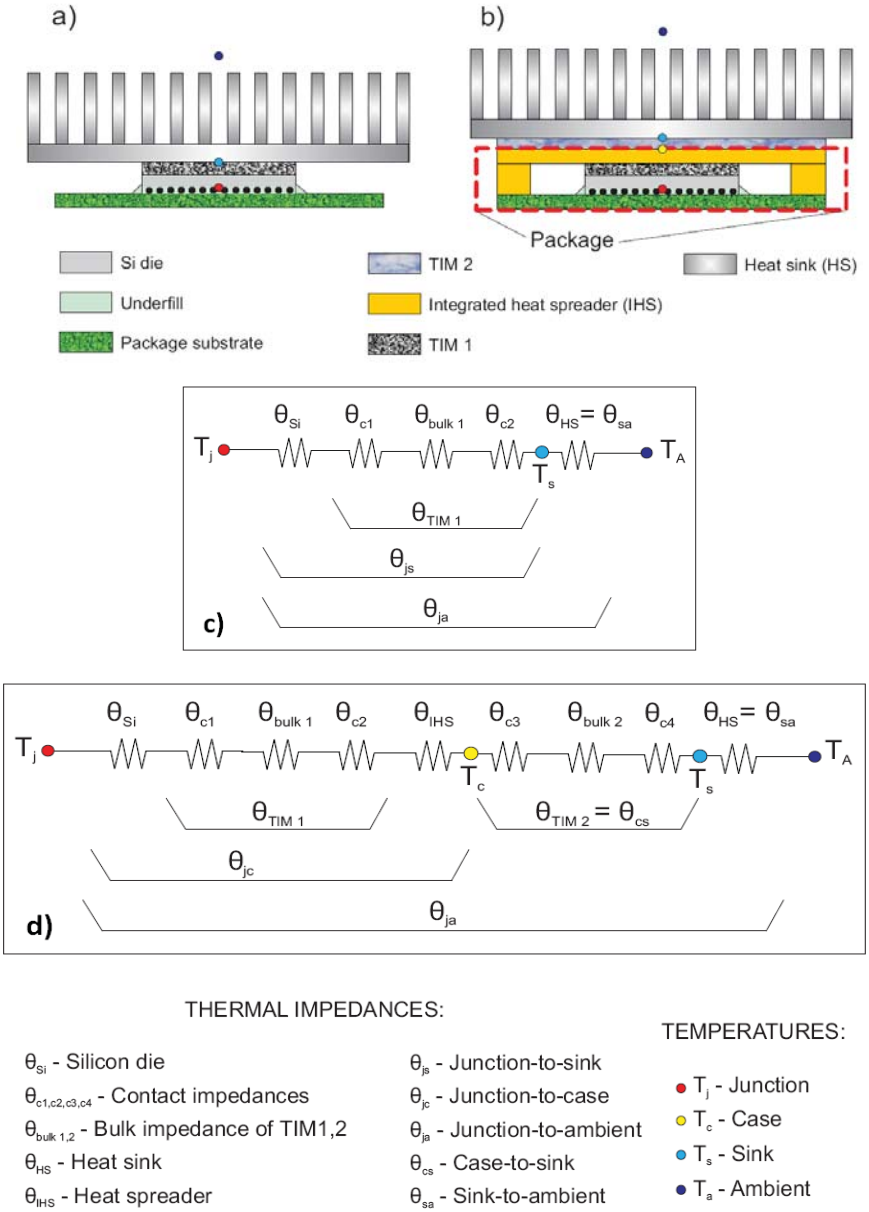

Fig. 2. (a-b) shows two sketches of a microprocessor package assembly used in a real application scenario of electronics cooling, respectively for past and more recent desktop applications. Here, the superimposition of different layers of materials in order to build the assembly leads to a creation of a thermal impedance chain as shown in Fig. 2(c-d) (Chiu 2006; Mahajan 2002; Prasher 2006; Sauciuc et al. 2005; Torresola et al. 2005; Xu 2006).

For convenience, by looking only at the sketches in Fig. 2(b) and (d), the heat transfer through the complete assembly involves the following three major stages (along with the respective thermal impedances) (Grujicic et al. 2005):

- Heat transfer within the device package (θjc).
- Heat transfer from the package to a heat sink (θcs).
- Heat transfer from the heat sink to the ambient environment (θsa).

The main bottlenecks in reducing the θja are the interfacial impedances between the package and the heat sink (Prasher 2006): this is due to the mating surfaces between the package and the heat sink, which, in the real application scenario, are generally neither fully conforming nor smooth and thus, leading to a significant increment of thermal contact impedance. Hence, the thermal management within the area of the chip is a relevant issue: Table 1 summarizes the ongoing challenges related to air cooling technology in order to minimize the junction-to-case thermal impedance.

Thermal impedance	Thermal management challenge
Junction-to-case	IC-level cooling
	Package architecture development
	Interface thermal contact impedance minimization
Case-to-heat sink	Interface thermal contact and TIM bulk impedance Minimization
Heat sink-to-ambient	Advanced heat sink manufacturing technologies
	Improvement of heat spreading technologies
	Integration of hybrid cooling solutions
	Aerodynamic fan performance improvement
	Airflow optimization
	Heat sink surface fouling minimization
	Sustainability

Table 1. Air-cooling solutions: thermal management key areas for improving the heat removal from the silicon die to the heat sink (Rodgers et al. 2005). The highlighted text shows the topic on which this study is focused.

In relation to this chapter, the research presented will focus on the case-to-heat sink impedance, in particular by looking at the thermal properties of TIMs and the way to accurately quantify the same. To this end, the following section reviews the recent progress of the research and industry work performed to develop new emerging materials and improve the existing state-of-the-art; furthermore, a variety of methods and their implementations used to characterize the TIMs are also introduced.

3. Review of nanowire/ nanotube based composites

Polymer nanocomposites can have potential microelectronic applications in a wide range of areas which includes resistors, inductors, capacitors, lasers, low loss dielectric, waveguide, thermal interface materials, etc. Most of these nanocomposites used nanoparticles and micro particles as filler materials to tune the physical and electrical or thermo-mechanical properties. The use of nanowires or high aspect ratio structures are recently been investigated. The use of high aspect ratio structures has one obvious benefit and that is its ability to achieve low percolation threshold in a nanocomposite compared to nanoparticles.

The down side is the composite material may not be as flexible as the nanoparticle infused nanocomposites. Carbon nanotube (CNT) nanocomposites may be the exception where due to its ultra high aspect ratio the tubes are flexible enough and until a certain percentage of inclusion the nanocomposites made using CNT as filler can have similar flexibility and modulus as nanoparticle filled nanocomposites.
Micro-and nano-boron nitride (BN) particles, aluminium nitride, aluminium oxide, silver and other metals act as thermal conductor in either silicone or epoxy compounds. Btechcorp has patented a process for aligning fine (8 μm diameter) continuous metallic fibres (Ni, 40% vol.) through the thickness of a polymer matrix (Btechcorp 2008). Arctic Silver invented a commercially-available paste made of high-density filling of micronised Ag and enhanced thermally conductive ceramic particles dispersed in a proprietary mixture of advanced polysynthetic oils, claiming a thermal conductivity as high as 8 $Wm^{-1}K^{-1}$ (ArticSilver 2010). Kempers et al. developed and characterised a novel metal micro-textured (MMT) TIM consisting of a thin metal foil with engineered conical micro-scale features which deform under clamping pressure and thus, creating a continuous thermal path between the contacting surfaces (Kempers et al. 2009a; Kempers et al. 2009b). Carlberg et al. introduced and characterised the thermal performance of a nanostructured polymer-metal composite which consists of high-porosity nanofiber network infiltrated with a low melting temperature alloy (Carlberg et al. 2008a; Carlberg et al. 2008b; Carlberg et al. 2009). Wunderle et al. developed and applied different surface modification methods to create the so-called "nano-sponge" in a thin Au layer (Wunderle 2010). A second technology using Ag-powder on Ag surface metallisation (sintering approach) has also been developed.

3.1 Nanotube composites

The urgent necessity of novel and high performance TIMs from the silicon devices companies has drawn the attention of researchers during the last decade (Liu et al. 2008a; Liu et al. 2008b). Therefore, TIMs based on carbon composition including CNTs, graphite; diamond and amorphous carbon are being studied among academic institutions and industry. The reason behind this is the great potential in term of thermal conductivity showed by the carbon allotropes (Melechko et al. 2005; Ngo et al. 2004). Worthwhile to mention research groups in the field of carbon-based TIM development are reported as follows: Purdue University are carrying on works on different methods of growing vertically aligned-CNTs along with new test approaches in developing the same (Cola et al. 2009; Cola et al. 2007a; Cola et al. 2007b; Xu and Fisher 2006). At Hong Kong University lift-off transfer of CNT films and development of Cu-CNT composite have been investigated (Chai et al. 2007a; Chai et al. 2007b; Chai et al. 2007c). At Tsinghua University CNT-PDMS (polydimethylsiloxane) composite by inject moulding has been invented (Huang et al. 2005). Also we have investigated different types of CNT-polymer to study the thermal properties of these nanocomposites (Razeeb et al. 2007; Xu et al. 2008).
Despite the great efforts put forward from the research, these new TIMs are unfortunately still far away from being available on the market because the performance exhibited is still not high enough to overtake the current best-in-class commercial products: this concept is also emphasised by the ITRS which predicts the earliest potential insertion of some cutting-edge materials for thermal management not sooner than 3-5 years. Many technical issues can be identified (Liu et al. 2008b). Theoretical predictions show that CNTs have extremely high thermal conductivity: these computations are mainly based on the assumption that

CNTs are ideal atomic structures, whereas in the real application scenario defects and impurities contribute to lowering their thermal conductivity. Furthermore, the contact thermal impedance between nanotubes and other substances, e.g. the polymer matrix in composites, is very high and even the functionalisation of CNTs is not sufficient to enhance consistently the performance of those composites. Also, CNTs have a high modulus of elasticity and when aligned in a vertical array, this may cause an increase in contact impedance with the substrates above and below the aligned array. Moreover, in the case of aligned structures, it is difficult to achieve high filling ratio, whereas in the case of using CNTs as filler for silicone or epoxy composites, their homogeneous dispersion in the polymer matrix would be more than a concern. Similar considerations apply for TIMs with other fillers than CNTs, where, the volume fraction and overall dimensions of the dispersed particles play a significant role in understanding how the heat will be conducted. More importantly, the ongoing research should focus on minimising the overall thermal impedance rather than improving the thermal conductivity of the composites based on theoretical models (percolation paths between particles in close contact) (Prasher 2006). Another negative aspect that contributes to uncertainties when comparing the performance of TIMs from different sources is that the materials are tested using different standard test methods. Also different implementations or modifications of the same standard may lead to discrepancies in results (Lasance et al. 2006).

3.2 Nanowire composites

In recent years there is a surge of publications in the area of metallic and semiconductor nanowire fabrication and applications as novel transistor device, sensors, biosensors, high density data storage, in energy scavenging, e.g. solar, thermoelectric, piezoelectric, etc. as well as semiconductor packaging materials to be used as z-axis interconnections, thermal interface materials, and so on. Similarly, a surge of publications was observed in the area of magnetic nanowires to explore the novel physics and material properties at reduced physical dimensions. In a recent publication, nickel nanowire and nanoparticles are used as filler materials in a nanocomposite fabrication using polydimethylsiloxane (PDMS) as polymer in order to investigate the magnetic properties of the nanocomposite (Heather et al. 2009; Sun and Keshoju 2008). For thermoelectric application, aligned Si nanowire were fabricated using vapour-liquid-solid (VLS) process and infused with low thermal conductivity and conformal polymer parylene. A thermal conductivity of 4.9±2.2 $Wm^{-1}K^{-1}$ was measured for the composite (Abramson et al. 2004). Similarly, bismuth telluride nanowire-epoxy composite were fabricated which showed reduced thermal conductivity and thereby a reduction in performance penalty from 27% to ~5% (Kalapi et al. 2009).

However, the use of nanowire composites as thermal interface materials seems to be limited to a few publications including ours. Recently, there are study to evaluate the complete set of effective transversely isotropic properties of a nanocomposite at various nanofiber-volume fractions through effective continuum modeling and experimental testing which used Co nanowires as filler materials. The study found significant anisotropy in the effective thermo- mechanical properties of the nanocomposite but surprisingly not in the effective Poisson's ratio and coefficient of thermal expansion (CTE) (Chen et al. 2008). Micrometer (5 and 10 μm) long Ag and Cu nanowires having a diameter of 25 nm fabricated using template based method mixed with polystyrene. The composites attained a low percolation at a 0.25 and 0.75 vol% (Gelves et al. 2006). Further study showed that unfunctionalized Cu

nanowires having a diameter of 25 nm and length 1.78 μm able to form electrical conductive networks at 0.5 vol% whereas for functionalized nanowires it is 0.25 vol%. The electrical resistivity of the percolated nanocomposites showed a value of 10^6–10^7 Ωcm (Gelves and et al. 2008). Similarly, the Ag nanowires electrical percolation behavior was studied using both simulation and experimentation by White et al. (White et al. 2010). The study of electrical and mechanical properties of nanocomposites at low volume fraction (0.1-7 vol%) of high aspect ratio structures is interesting. This is due to the ability of these nanotube/ nanowire fillers in achieving percolated network at a low volume fraction compared to spherical micron and nanoparticles.

In an attempt to increase the thermal conductivity of organic phase change materials 62.73 wt% of Ag nanowires are infused in 1-Tetradecanol. A thermal conductivity of 1.46 $Wm^{-1}K^{-1}$ was achieved at a high phase enthalpy of 76.5 Jg^{-1}, which was attributed to the high aspect ratio of the nanowires in the composite PCM (Zeng et al. 2009). Similarly, Ni NW/P(VDF-TrFE) composites were prepared with a volume fraction of Ni nanowires varying from 0 to 5 vol %, achieving an electrical percolation threshold at 0.75 vol%. An electrical conductivity of 10^2 Sm^{-1} was observed for the composites using nanowires with aspect ration ~250 (Lonjon et al. 2009). Munari et al. also applied a similar approach where silver nanowires were fabricated using a polyol process and mixed with silicone elastomer (PSW 2286) using different wt% of nanowire up to a value of 7.2. A thermal impedance of 2.6 $°Ccm^2W^{-1}$ was achieved at a pressure of 0.6 MPa with a bond line thickness of 0.5 mm. In this study, length of nanowires fabricated using polyol method has a wide variation typically ranging from 10-50 μm with an average wire diameter of 100 nm (Munari et al. 2009). In a different approach, rather than mixing the nanowires at a high wt%, we used polymer template to grow nanowires through the pores. Individual nanowires should be able to contact the heat generating and the dissipating devices and thereby with lower concentration of filler materials (Ju et al. 2009; Razeeb and Roy 2008) low impedance should be achieved. One of the interesting works which achieved low thermal impedance reported a different TIM structure, where electrospun porous polymer fiber was coated with multi-layer Ni/Au layer. This was further coated with Field's metal alloy (InBiSn) which has a melting point of ~60 °C by force infiltration to create the composite film. A thermal impedance of 8.5×10^{-2} $°Ccm^2W^{-1}$ was reported at a pressure of 0.8 MPa with a bond line thickness of 70 μm (Carlberg et al. 2009).

4. Nanowire composites as thermal interface materials

As semiconductor device feature sizes continue to be reduced, ensuring reliable operation has become a growing challenge. The effective transfer of heat from an integrated circuit (IC) and its heat spreader to a heat sink is a vital step in meeting this challenge (Cola et al. 2008). Microscopic surface roughness and non-planarity of the IC/heat spreader and heat sink surfaces result in asperities between the two mating surfaces, which prevent the two solids from forming a thermally perfect contact due to the poor thermal conductivity of air that exists in the gaps between the two surfaces (Prasher et al. 2003). Thermal interface materials (TIM) are, therefore, used to provide an effective heat conduction path between the two solid surfaces owing to their conformation to surface roughness and high thermal conductivity (Razeeb and Roy 2008). Different TIMs such as metallic foils, grease, phase change materials, adhesives, elastomer and thermoplastic polymers have already been

deployed for reducing the thermal impedance between joints (Savija et al. 2003), The thermal impedance of this system is comprised of the combined thermal contact impedances of the two surfaces and the bulk thermal impedance of the TIM material. Elastomer and thermoplastic polymer TIM composites made of a low modulus polymer matrix and high thermally conductive particle fillers are already widely used. The typical thermal impedance between joints is above 1.0 °Ccm^{2}W^{-1} when using traditional particle-laden elastomeric pads (Viswanath et al. 2000). However, TIMs with lower thermal impedance are required, according to the 2007 ITRS roadmap (ITRS 2007). Recently, advanced thermal management schemes using carbon nanotubes (CNTs) as filler particles in polymer or CNT arrays directly as TIMs have been suggested as a means to dissipate high heat fluxes while maintaining low chip temperatures. These proposals have been made on the basis of the high intrinsic thermal conductivity of CNTs (Prasher 2006). So far, the reported effective thermal conductivity of CNT arrays range from 74 to 83 Wm^{-1}K^{-1}, and the lowest thermal impedance between substrates obtained by using CNT array based TIMs is about 0.1 °Ccm^{2}W^{-1} which is an order of magnitude lower than the commercial elastomeric pad TIMs (Cola et al. 2007b). However, while using the CNT arrays as TIMs has the potential to compete with state-of-art thermal pads, the fabrication of these CNT array thermal interfaces requires high temperature (above 800 °C) processes and these are incompatible with the temperature-sensitive substrates used in most semiconductor technologies. Furthermore, the electrical performance of most metal contacts and interconnects degrades when exposed to a temperature in excess of to 450°C for more than a very limited time (Cola et al. 2007b). Using *insertable* CNT array as a TIM has also been reported. However, in this case the contact impedance between the CNTs and substrates was found to be high. This was associated with non-uniform growth of CNTs preventing all of the CNTs in the film from making proper thermal contact to the opposing surface. Furthermore, the high Young's modulus of CNTs (0.8~0.9 TPa for multi-wall-CNTs, 1~5 TPa for single-wall-CNTs (Srivastava et al. 2003)) prevents the array from conforming between surfaces and achieving good thermal contact (Cola et al. 2007b; Schelling et al. 2005). The possibility of inadvertently incorporating contaminating impurities, the existence of voids between CNTs, and the growth conditions of CNT arrays greatly affect the effective thermal conductivity of CNTs, typically resulting in a TIM with a large performance uncertainty. In addition, the need for mass production due to the high commercial volumes requirement and the high cost of fabrication may be another hindrance to the industrial acceptance of this solution.

In this work, we investigate a polymer composite which uses silver nanowire (AgNW) arrays - as opposed to CNT array - in a TIM. These nanowires have an average diameter of 220 nm and an aspect ratio of >100. Bulk silver has an excellent thermal conductivity of 429 Wm^{-1}K^{-1} and it has a low Young's modulus of 83 GPa, which is far lower than that of CNTs (800 GPa). This suggests a better conformability to the rough surface of the substrates, and may permit achievement of superior thermal impedance than CNT-based TIMs. Furthermore, compared to the Ag particles/flakes which have already been widely used as fillers for many polymeric TIMs, the AgNW arrays are expected to be better effective thermal conduits due to their inherent continuity, vertically-aligned orientation and their ability to conform to micron-scale unevenness of the mating surfaces. Nanoporous polymer template can be used to fabricate these high aspect ratio nanowires by the electrodeposition techniques. However, thermal conductivity and, particularly, thermal impedance of these AgNW-polymer composites have not yet been reported. Furthermore, a comparison of aligned AgNW-polymer and CNT-polymer TIMs is necessary in order to understand the

thermal contact impedance behaviour of these two composites. As discussed above, thermal contact impedance characteristics are the performance defining parameter for any thermal interface material.

5. Fabrication and characterization of nanowire-polymer nanocomposites

5.1 Sample fabrication and material characterization

The AgNW - polymer composite was fabricated by electrodeposition using a porous polycarbonate (PC) film (Millipore, pore density: ~20%, pore diameter: ~220 nm) as a template. Typically, a 100 nm Ag thin film was deposited at the bottom of the template to act as a seed and conductive layer. A bath comprising 50 gl^{-1} $AgNO_3$ and 200 gl^{-1} CH_3COONH_4 was prepared. Deionized water with resistivity ~18 MΩ was used to prepare the solution. Electrodeposition was performed with stirring at a constant 500 RPM. A current density of 1 $mAcm^{-2}$ was applied and all the deposition was performed at room temperature. After deposition, the samples were thoroughly rinsed with deionized water; any Ag overgrowth was removed manually and dried with a nitrogen gun. After thermal impedance measurements of the as prepared samples, the top surface of the samples was coated with a 30 nm Au film by e-beam evaporation. This was to investigate the influence of a conductive metal layer on overall thermal impedance of the nanocomposite material. The top surface and the cross-sectional view of the AgNWs within the PC matrix were characterized by scanning electron microscopy using a JOEL 200 SEM. For an estimation of overall grain size and crystal orientation, X-ray diffraction (XRD) measurements were carried out using a Philips PW3710 diffractometer with Cu-$K\alpha_1$ radiation that had a wavelength of 1.540598 Å.

5.2 Thermal diffusivity measurements

Thermal diffusivity measurement of the AgNW-PC composites was carried out using the laser flash method (Parker et al. 1961; Razeeb and Roy 2008). A short laser pulse (using Nd:YAG laser) of duration 7 ns was applied to the samples to create an effectively instantaneous heat source. The Ag seed layer side was heated with the laser pulse where the diameter of the laser beam was 4 mm. An infrared detector was positioned on the opposite side of the sample to where the pulse impinged in order to measure the thermal response that is generated during this illumination. The resulting rise in temperature was recorded using the pre-amplifier and oscilloscope setup, which was controlled using a Labview program. In this method, heat flow is assumed to be one-dimensional in the direction perpendicular to the planar surfaces. The duration of the pulse is short enough to be considered effectively instantaneous in comparison to the time taken for the thermal response to reach half of its maximum value. The time at which the curve reaches that value is given by the following equation:

$$t_{0.5} = \frac{1.38l^2}{\pi^2 \alpha} \tag{2}$$

where α is thermal diffusivity, l is thickness of the sample and $t_{0.5}$ is the time at which the thermal response at the opposite side of the sample reaches half of its maximum value. Diffusivity is calculated from the time $t_{0.5}$ and the thickness of the samples. All the measurements were conducted in air and therefore heat loss correction for radiative and convective heat losses was done according to Cowan (Cowan 1963).

5.3 Thermal impedance measurements

To measure the thermal impedance of the composites, a modified ASTM D5470-06 standard setup was employed (Munari et al. 2009; Razeeb et al. 2007). A detailed drawing of the experimental setup can be seen in Fig. 3(a), where different components are numbered to describe the setup. The meter bars (7) are made of two round copper C11600 rods 60 mm-long and 20 mm-diameter and have a nominal thermal conductivity of 388 $Wm^{-1}K^{-1}$ at 25 °C. The contact surfaces were ground with a Buehler grinder apparatus and polished with 1 micron diamond paste to get a mirror finish. The surface roughness was measured with an NT-MDT model atomic force microscope (AFM). Fig 3(c) and (d) show the representative topographic and the 3D topographic images of the surface of copper calorimeter, which showed an RMS (root-mean-square) roughness of 88 nm. Eight 0.5 mm diameter thermistors were embedded within the bars to measure the thermal gradients with an accuracy of ±0.01 °C, between 0-70 °C. Calibration of the thermistors was performed with a Hart Scientific 5611T model reference probe with an absolute calibrated uncertainty of 0.002 °C. The thermistor resistances were recorded using two National Instruments DAQ-mx USB cards, each equipped with 4-channels and each in 4-wire resistance configuration using a built-in low excitation current. Cooling of the lower meter bar was provided by a Lauda thermal bath constant-temperature cooler loop whose stability was ±0.02°C. The upper meter bar was heated using an aluminium heater block with two internal 250 W cartridge heaters controlled by a Red-Lion PID controller. The heater block was attached to an AST KAF-S Load Cell with rated load of 2 kN ±0.2% (11). The load cell, in turn, was then attached to Nanotec Ball Screw Linear Actuator, which can apply a maximum force of 1.8 kN onto a surface of 3.14×10^{-4} m^2. Furthermore the actuator has a minimum step size of 1 µm resolution (15). The distance between the two mating surfaces of the bars was measured using an MX-Metralight laser micrometer with a 0.4 µm resolution (10) and thereby the bond line thickness (BLT) of the sample could be measured in situ. During testing, the meter bars were wrapped in an insulating material (not shown in Fig. 3) to minimize heat losses.

Calibration of the test facility was carried out by machining 4 stainless steel (303 grade) disks with different thicknesses. According to data sheets provided by the manufacturer, a nominal thermal conductivity of 15.10 $Wm^{-1}K^{-1}$ is expected at 29.27 °C, which is the mean temperature of the sample under test. Prior to testing, a thin layer of highly conductive thermal paste was spread onto both faces of the disk in order to minimize contact impedance as much as possible, because this differs from sample to sample depending on surface roughness. Each disk was compressed between the meter bars under a constant contact pressure of 1 MPa and the thermal impedance of the disk was measured. These measurements are plotted in Fig. 4 against their respective thicknesses. A linear fit is used for this set of data and the slope is equal to the inverse of the thermal conductivity of the bulk material. The effective thermal conductivity according to this simple calculation is found to be 15.01 $Wm^{-1}K^{-1}$ which is within 0.59% of the manufacture's value of 15.10 $Wm^{-1}K^{-1}$.

6. Nanowire-polymer composite as TIM

The SEM images of Fig. 5 indicate that the *as-grown* Ag arrays are vertically aligned. The top view of the nanocomposite film shows that AgNW have extruded outside the polycarbonate membrane. It should be noted that the wires were distorted while preparing the sample for cross section analysis as shown in the inset of Fig. 5(a). The nanometer-size of these AgNW tips are expected to be able to conform to the submicron roughness of the substrate surfaces. Fig. 5(b) shows the high magnification image of the top surface where the grains of the AgNW are visible.

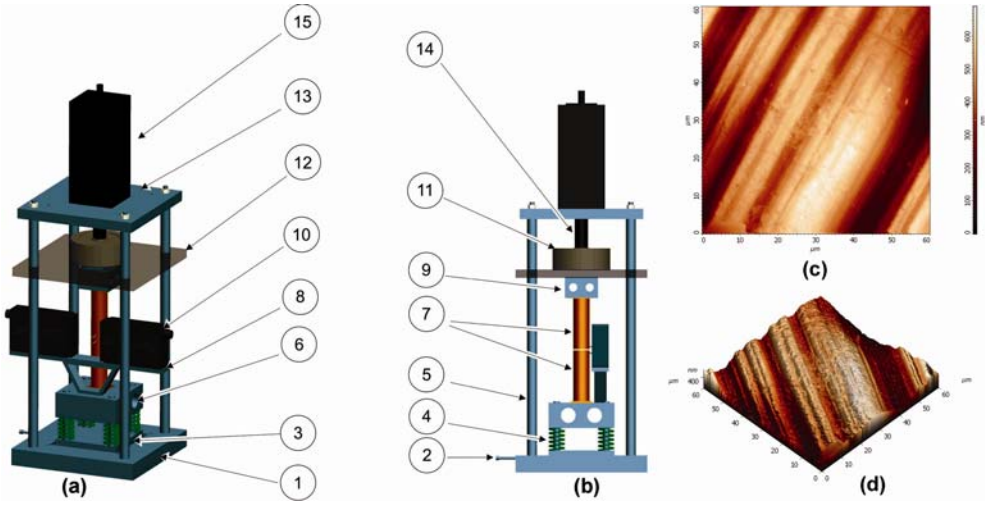

Fig. 3. Cad design of the experimental apparatus. (a) Front view and (b) side view of the apparatus. (1) Aluminium plate (2) Fine threaded linear screw for x-y displacement. (3) Insulating Perspex plate, (4) Compression springs, (5) Aluminium shafts, (6) Aluminium cooler block, (8) Micrometer stand, (12) Perspex plate. (13) Steel plates. (14) Stainless steel Ball-Screw. (c) and (d) show the representative topographic and the 3D topographic images of the surface of copper calorimeter.

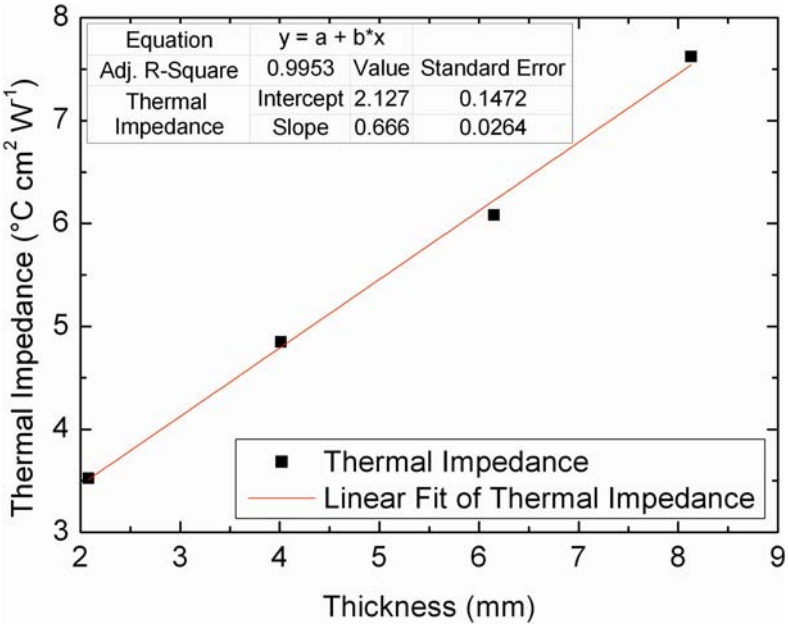

Fig. 4. Measured thermal impedance versus thickness of 303-Stainless steel disks.

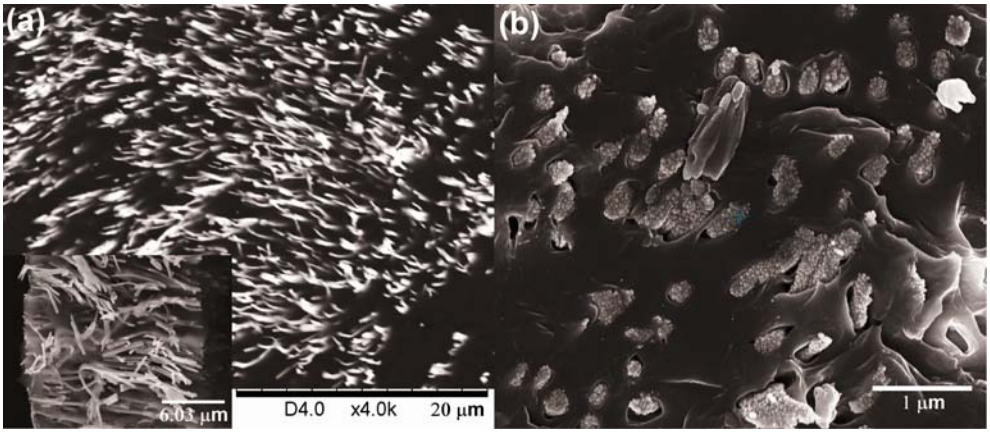

Fig. 5. SEM images of AgNW arrays within PC matrix. (a) Top surface showing nanowires coming out of pores. Inset showing cross section, (b) top view (Ju et al. 2009).

The real filling ratio (φ) of AgNW within the PC membrane was calculated according to the following formula:

$$\varphi = \frac{V_{Ag}}{V_T} = \frac{(W_2 - W_1)/\rho_{Ag}}{\pi D^2 h / 4} \tag{3}$$

where V_{Ag} is the volume of AgNW, V_T is the total volume of the PC membrane which includes unfilled pores, W_1 is the weight before deposition and W_2 is the weight of the sample after the Ag plating process, ρ_{Ag} is the density of silver, D is the diameter of deposited area and h is the thickness of the membrane. A filling ratio of 9 vol% AgNW was obtained for the samples studied in this work.

According to the rule of mixtures for a simple parallel model, the effective thermal conductivity in the z direction is (Razeeb and Roy 2008):

$$k_z = k_m(1-\varphi) + k_p\varphi \tag{4}$$

where k_z is the thermal conductivity of the composite material along the z direction, i.e. perpendicular to the sample surface, k_m and k_p are the bulk thermal conductivities of the matrix and the AgNW, respectively, and ϕ is the volume percentage of the AgNW in the composite. Considering that the bulk thermal conductivity of polycarbonate is 0.2 $Wm^{-1}K^{-1}$ and Ag is 429 $Wm^{-1}K^{-1}$, the calculated thermal conductivity of this composite is shown in Fig. 6, as a function of volume concentration of AgNW. The porosity of PC membrane is ~20%. Therefore, in case of 100% pore filling, the volume percentage of AgNW will be 20% in the polymer matrix. The calculated thermal conductivity value of this AgNW-PC composite is ~86 $Wm^{-1}K^{-1}$, which is comparable to CNT arrays (74-83 $Wm^{-1}K^{-1}$).

The thermal conductivity of the AgNW-PC composite was determined from the thermal diffusivity values, measured using the laser flash method described in section 5.2 and other works (Razeeb and Roy 2008). Fig. 7 shows the thermograms of silver foil (purity 99.99%, thickness 265 µm), PC template (with a thickness of 24±1 µm), before Ag nanowire formation (PC without AgNW) and after fabrication of AgNW-PC (thickness 24 µm). The

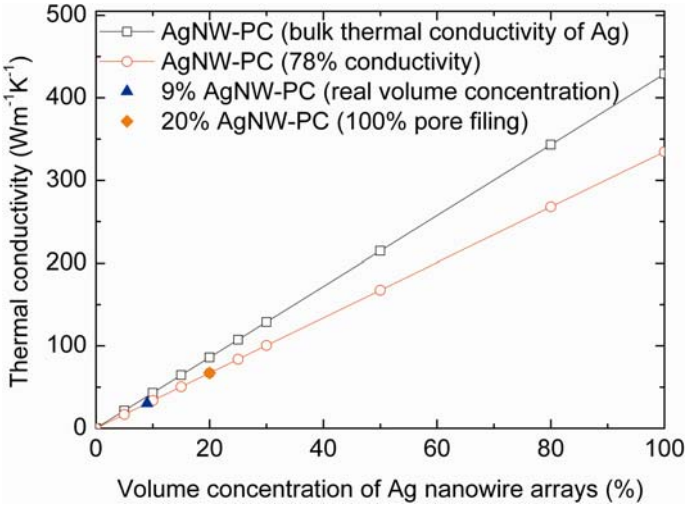

Fig. 6. Thermal conductivity of AgNW-PC nanocomposite as a function of vol.% of Ag (Ju et al. 2009).

blank PC membrane with Ag seed layer on one side resulted in a thermal diffusivity of 0.0152×10^{-5} m^2s^{-1} and pure Ag foil (265 μm thickness) showed a diffusivity value of 17.356×10^{-5} m^2s^{-1}. These values represent differences of 1.6% and 0.17% respectively, when compared to values of polycarbonate and silver in the literature (Weast 1994). The values obtained for the composite varied from 1.82×10^{-5} to 1.96×10^{-5} m^2s^{-1} and showed an average value of 1.89×10^{-5} m^2s^{-1}. This shows a significant increase in the diffusivity of the composite to that of blank PC a factor of 124.

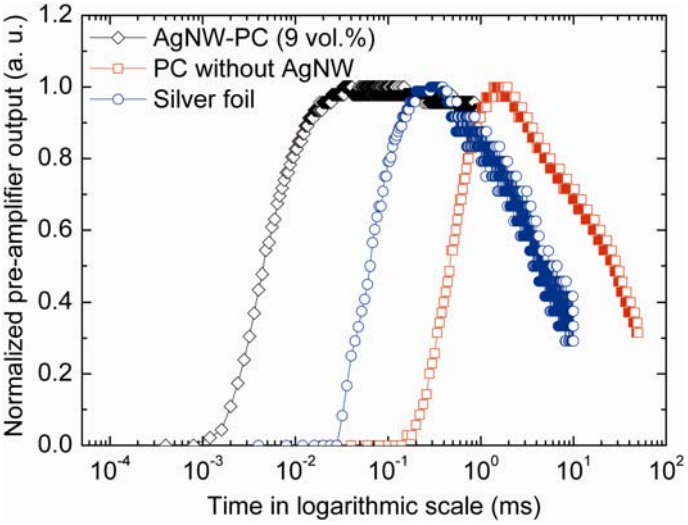

Fig. 7. Thermal transients of AgNW-PC, PC template without AgNW and silver foil (Ju et al. 2009).

Combining with the experimental thermal diffusivity value, the Eq. (4) can be written as,

$$k_{NC} = k_{PC}(1-\varphi) + k_{Ag}\varphi = \alpha[(\rho c)_{PC}(1-\varphi) + (\rho c)_{Ag}\varphi] \quad (5)$$

where k is the thermal conductivity and (ρc) is heat capacity per unit volume. φ is the volume percentage of Ag in the composite and α is the thermal diffusivity of the composite. For 9% filling ratio of AgNW (as achieved in this paper), the calculated thermal conductivity is ~38.8 $Wm^{-1}K^{-1}$ according to equation 4. However, a thermal conductivity of 30.3 $Wm^{-1}K^{-1}$ was evaluated (using Eq. 5) for the nanocomposite using the experimental diffusivity value and considering the density and the heat capacity of silver and polycarbonate. It is interesting to note that the calculated thermal conductivity value of the nanocomposite (k_{NC}) (38.8 $Wm^{-1}K^{-1}$) using the modified effective medium theory, over-predicted the experimental values when the bulk thermal conductivity of Ag was considered. However, when the thermal conductivity of Ag was reduced to ~78% of the bulk conductivity, the theoretical value showed excellent correspondence. In this case, AgNW have an effective thermal conductivity of 334.6 $Wm^{-1}K^{-1}$. In order to understand this conductivity reduction, an XRD analysis was carried out on AgNW samples. The XRD analysis revealed that the AgNW are polycrystalline with a preferred orientation of (111). The *Scherrer* formula was employed to calculate the grain size of the AgNW, which showed an average grain size of 204 nm. A similar reduction in conductivity value for Ni nanowires has already been observed as an effect of grain size (Razeeb and Roy 2008). The deviation from bulk thermal conductivity in case of AgNW may be explained as follows: The thermal conduction in pure metals is usually dominated by electron rather than phonon conduction. Therefore, the thermal conductivity and diffusivity are dominated by the scattering process of conducting electrons. At room temperature, the electron mean free path of Ag is 52 nm (Zhang et al. 2004). Although the average grain size obtained from XRD measurements is 4 times the mean free path of the electron, it was reported that the grain size of electrodeposited silver NW could vary from ~10 to ~200 nm (Kazeminezhad et al. 2007). In electrodeposited AgNW, there are also large numbers of defects and dislocations in crystals and, therefore, the grain boundary scattering of conduction electrons is believed to be responsible for the reduction in measured thermal conductivity over the expected theoretical value.

In a publication by Huang et al. (Huang et al. 2009) it was shown that the electrical resistivity of a single crystalline trapezoidal silver Ag nanowire is dominated by the electron diffusely scattering on the nanowire surface and explained their experimental results using Chamber's approach (Chambers 1950) to the FS (Fuchs and Sondheimer) theory (Fuchs 1938; Sondheimer 1952). Their work was focused to differentiate the surface scattering from the grain boundary scattering and for single crystal wires the experimental resistivity fit well to the theoretical resistivity models that are close to purely diffuse surface scattering. Durkan et al. (Durkan and Welland 2000) on the other hand, argued that in a polycrystalline wire, when the wire width is comparable to the average grain size, the grain boundary scattering is the dominant source of increased resistivity. Only when the wire width is below ~0.5 times the grain size, surface scattering becomes important and approaches to the same order of magnitude of grain boundary scattering. Similarly, it was observed that the surface scattering is intimately connected with the geometrical dimensions, i.e. diameter of the wires. This scatting becomes important when the diameter is comparable to or smaller than the mean free path of the conduction electrons of the respective metal (Steinhögl et al. 2002). In the present case, the nanowires are polycrystalline with an average grain size is ~204 nm

and have a diameter of 220 nm, which is comparable to the grain size. Thereby, the grain boundary scattering will be the dominant factor in reducing the thermal diffusivity and conductivity of the Ag nanowires, rather than surface scattering.

The thermal impedances of the as-prepared AgNW-PC composite films with (AgNW-PC-top metal layer) and without the top metal layer (AgNW-PC) are shown in Fig. 8 as a function of applied contact pressure. To facilitate comparison, a blank PC template, with a 100 nm Ag seed layer and a commercially-available thermal pad are also included. The thermal impedance of the PC membrane before and after seed layer deposition did not show a large variation, specifically when the contact pressure exceeded 0.2 MPa. In the lower contact pressure range, the seed layer acted as a heat spreader and enhanced the heat transfer, which resulted in a further reduction of measured thermal impedance. However, as the contact pressure was increased, this effect diminished. The thermal impedance of the AgNW-PC composite sample showed at least a 61% reduction compared to the PC with seed layer under all measured contact pressures and a 29% reduction compared to commercial thermal pad. When a 30 nm Au film was deposited on top of the AgNW-PC film, the thermal impedance was reduced by another 35%, to 0.93 °Ccm^{2}W^{-1} at a contact pressure of 1.0 MPa. The SEM analysis on different areas of the AgNW-PC samples revealed that not all of the nanowires came out of the pores due to non-homogeneity in the pore structure. The deposited Au film effectively connected most of the nanowires together and thereby increased the effective contact area. As a result, the thermal impedance decreased, which was also reported for carbon nanotube arrays (Panzer et al. 2008; Wu et al. 2005). This limiting of contact area (without top metal layer) leads to an increase in the contact impedance, ultimately increasing the overall impedance of the TIM. The contribution of contact impedance will be explored in section 7.

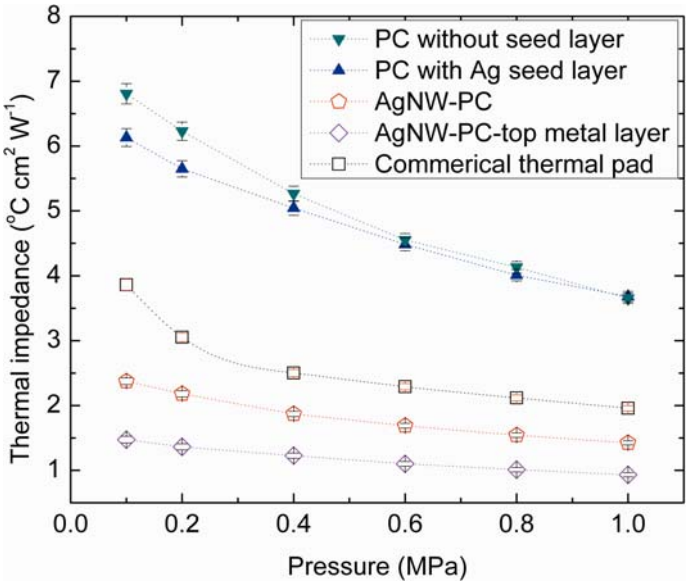

Fig. 8. Thermal impedance (with error bars) of AgNW-PC composite and reference samples as a function of contact pressure (Ju et al. 2009).

7. Contact impedance model

The two most important parameters for a thermal interface material is its thermal contact impedance and bulk conductivity. The following section employs a thermal impedance model (Singhal et al. 2004) to explore how these two parameters affect the thermal impedance as a function of decreasing bond line thickness for both aligned AgNW and aligned CNT embedded in a polycarbonate matrix. With decreasing bond line thickness, the percentage contribution of the contact to overall thermal impedance increases and is of critical importance to the thermal behaviour of an interface material. According to Singhal et al. (Singhal et al. 2004), the thermal contact impedance of two mating surface can be calculated from Eq. 6:

$$R_C = \frac{1}{1.55}\left(\frac{\sigma}{\tan\theta}\right)\left[\frac{E_{NC}\tan\theta}{\sqrt{2p}(1-v_e^2)}\right]^{0.94}\frac{1}{2}\left(\frac{1}{k_1}+\frac{1}{k_{NC}}\right) \quad (6)$$

where p is the contact pressure, σ is the RMS surface roughness, tanθ is the average slope of the asperities of the two contact surfaces and is equal to $0.125\sigma^{0.402}$, k_1 and k_{NC} are the thermal conductivity of the mating surface and composite respectively, v_e is the Poisson's ratio and E_{NC} the Young's modulus of the composite. In this case, the mating surfaces are the composite's surface and the surface of a copper calorimeter (used in the thermal impedance measurement) with a RMS roughness of 88 nm.
A modified effective medium theory (Eq. 4) is used to calculate the equivalent elastic modulus and effective Poisson's ratio of both the composites. The thermal conductivity of the CNT-polycarbonate composite is calculated by Eq. 7, developed by Nan et al. (Nan et al. 2003):

$$k_e = \left(1+\frac{fk_c}{3k_m}\right)k_m \quad (7)$$

where k_e is the effective conductivity of the composite, k_c and k_m the thermal conductivity of the CNT and matrix respectively and f the fractional volume content of the CNTs. The effective thermal conductivity of the AgNW-PC is taken as 30.3 $Wm^{-1}K^{-1}$ from the thermal diffusivity measurements. It should be noted that for these calculations an intrinsic thermal conductivity of 6000 $Wm^{-1}K^{-1}$ is used for the CNTs. However it is has been shown that aligned CNT material has generally a far lower thermal conductivity value (Gogotsi 2006), typically 3000 $Wm^{-1}K^{-1}$. The parameters and the associated values used in the contact impedance model are shown in Table 2.

Materials	Young's Modulus (Pa)	Poisson's Ratio	Thermal conductivity ($Wm^{-1}k^{-1}$)
Copper calorimeter	117×10^9	0.37	388
Silver	83×10^9	0.37	429
Polycarbonate	2.3×10^9	0.37	0.2
CNT	80×10^{10}	0.08	6000
Silver-polycarbonate composite	6.3×10^9	0.37	38.8 9% vol. of AgNW
CNT-polycarbonate composite	4.5×10^{10}	0.35	180 9% vol. of CNT

Table 2. Values used in contact impedance calculations (Ju et al. 2009; Weast 1994).

As can be seen from Fig. 9(a), AgNW-PC has a significantly lower contact impedance than that of the aligned CNT-PC, for all contact pressure ranges up to 1 MPa. Although there is an increase in the thermal conductivity of the polycarbonate matrix by the introduction of the CNT's, the increase in the contact impedance due to the stiffening of the composite essentially diminishes much of the gain. Since the Young's modulus of the silver used in the polycarbonate is an order of magnitude lower than that of CNTs, AgNW-PC composite does not suffer from this problem to the same extent. It was also observed that if the bond line thickness of the material is increased; the contact impedance becomes less of a concern in the overall (total) thermal impedance of the composite. This is shown in Fig. 9(b) (at a set contact pressure of 0.5 MPa) and, as would be expected, the CNT-polycarbonate composite surpasses the AgNW composite at the larger bond line thickness, in this case at 0.95 mm. This essentially showing that for thinner TIM, the most important aspect is the Young's modulus and not the intrinsic thermal conductivity.

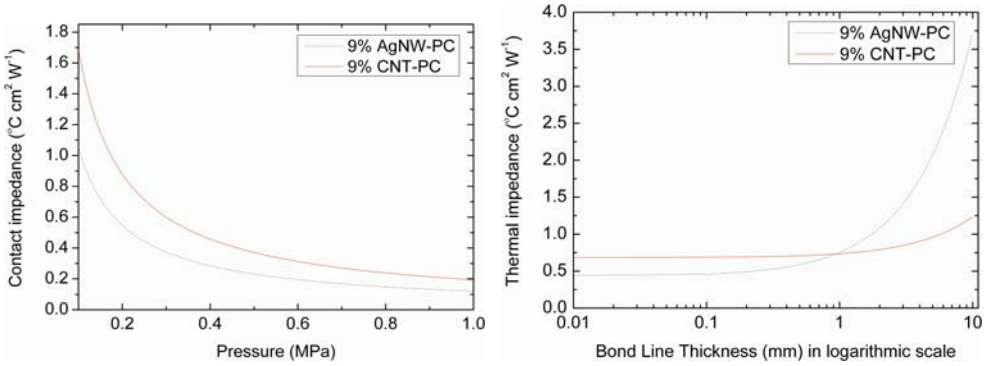

Fig. 9. (a) Contact impedance produced by 9% volume loaded AgNW aligned in a polycarbonate matrix (9% AgNW-PC) and aligned 9% volume loaded CNT in a polycarbonate matrix (9% CNT-PC) as a function of contact pressure, with a fixed bond line thickness of 30 μm. (b)Thermal impedance produces by 9% volume loaded AgNW aligned in a polycarbonate matrix (9% AgNW-PC) and aligned 9% volume loaded CNT in a polycarbonate matrix (9% CNT-PC) as a function of bond line thickness at a fixed contact pressure of 0.5 MPa (Ju et al. 2009).

8. Conclusion

Silver nanowire arrays embedded inside polycarbonate templates are investigated as a viable thermal interface material (TIM) for electronic cooling applications. The composite shows an average thermal diffusivity value of 1.89×10^{-5} m^2s^{-1}, which resulted in an intrinsic thermal conductivity of 30.3 $Wm^{-1}K^{-1}$. The protrusion of nanowires from the polymer film surface enables it to conform to surface roughness and this result in a reduction in thermal impedance of 61%, when compared to a blank template. A thin Au film on the top of the composite was found to act as a heat spreader, which further reduced the thermal impedance value by 35%. With emphasis on the contact impedance influence on the overall thermal impedance, it is shown through the contact impedance model that, for any thermal interface material, when there is decrease in the thickness; the Young's modulus becomes the dominant factor as opposed to its intrinsic thermal conductivity.

9. References

Abramson, A.R., Woo Chul, K., Huxtable, S.T., Haoquan, Y., Yiying, W., Majumdar, A., Chang-Lin, T., Peidong, Y., (2004). Fabrication and characterization of a nanowire/polymer-based nanocomposite for a prototype thermoelectric device. *Journal of Microelectromechanical Systems*, 13, 3, (505-513), 1057-7157

ArticSilver, 2010. Arctic silver 5. http://www.arcticsilver.com/as5.htm

Btechcorp, 2008. Highly electrically and thermally conductive z-axis film adhesives. http://www.btechcorp.com/index.html

Carlberg, B., Teng, W., Yifeng, F., Liu, J. (2008a). Preparation of polymer-metal nanocomposite films and performance evaluation as thermal interface material. *2nd Electronics System-Integration Technology Conference, 2008. ESTC 2008*, pp. 1395-1400, 978-1-4244-2813-7, Greenwich, London

Carlberg, B., Teng, W., Yifeng, F., Liu, J., Dongkai, S. (2008b). Nanostructured polymer-metal composite for thermal interface material applications. *58th Electronic Components and Technology Conference, 2008. ECTC 2008*, pp. 191-197, 0569-5503, Lake Buena Vista, Florida

Carlberg, B., Wang, T., Liu, J.H., Shangguan, D., (2009). Polymer-metal nano-composite films for thermal management. *Microelectronics International*, 26, 2, (28-36), 1356-5362

Chai, Y., Gong, J., Zhang, K., Chan, P.C.H., Yuen, M.M.F. (2007a). Low Temperature Transfer of Aligned Carbon Nanotube Films Using Liftoff Technique. *57th Electronic Components and Technology Conference, 2007. ECTC '07*, pp. 429-434, 0569-5503, Reno, NV

Chai, Y., Gong, J.F., Zhang, K., Chan, P.C.H., Yuen, M.M.F., (2007b). Flexible transfer of aligned carbon nanotube films for integration at lower temperature. *Nanotechnology*, 18, 35, (5), 0957-4484

Chai, Y., Zhang, K., Zhang, M., Chan, P.C.H., Yuen, M.M.F. (2007c). Carbon Nanotube/Copper Composites for Via Filling and Thermal Management. *57th Electronic Components and Technology Conference, 2007. ECTC '07*, pp. 1224-1229, 0569-5503, Reno, NV

Chambers, R.G., (1950). The Conductivity of Thin Wires in a Magnetic Field. *Proceedings of the Royal Society of London. Series A. Mathematical and Physical Sciences*, 202, 1070, (378-394), 0080–4630

Chen, W.-H., Cheng, H.-C., Hsu, Y.-C., Uang, R.-H., Hsu, J.-S., (2008). Mechanical material characterization of Co nanowires and their nanocomposite. *Composites Science and Technology*, 68, 15-16, (3388-3395), 0266-3538

Chiu, C.-P., 2006. Design and challenges of TIM1 for high-performance microprocessors. *Technical report*, Intel Corporation, Chandler, AZ, USA.

Cola, B.A., Amama, P.B., Xu, X.F., Fisher, T.S., (2008). Effects of growth temperature on carbon nanotube array thermal interfaces. *Journal of Heat Transfer-Transactions of the ASME*, 130, 11, (4), 0022-1481

Cola, B.A., Xu, J., Fisher, T.S., (2009). Contact mechanics and thermal conductance of carbon nanotube array interfaces. *International Journal of Heat and Mass Transfer*, 52, 15-16, (3490-3503), 0017-9310

Cola, B.A., Xu, X.F., Fisher, T.S. (2007a). Design, Synthesis, and Performance of a Carbon Nanotube/Metal Foil Thermal Interface Material. *ASME Conference Proceedings*, pp. 133-136, 0-7918-4265-7, Sanya, Hainan, China

Cola, B.A., Xu, X.F., Fisher, T.S., (2007b). Increased real contact in thermal interfaces: A carbon nanotube/foil material. *Applied Physics Letters*, 90, 9, (093513), 0003-6951

Cowan, R.D., (1963). *Journal of Applied Physics*, 34, 4, (926), 0021-8979

Durkan, C., Welland, M.E., (2000). Size effects in the electrical resistivity of polycrystalline nanowires. *Physical Review B*, 61, 20, (14215), 1098-0121

Fuchs, K., (1938). The conductivity of thin metallic films according to the electron theory of metals. *Mathematical Proceedings of the Cambridge Philosophical Society*, 34, 01, (100-108), 0305-0041

Gelves, G., Lin, B., Sundararaj, U., Haber, J., (2006). Low Electrical Percolation Threshold of Silver and Copper Nanowires in Polystyrene Composites. *Advanced Functional Materials*, 16, 18, (2423-2430), 1616-3028

Gelves, G.A., et al., (2008). Electrical and rheological percolation of polymer nanocomposites prepared with functionalized copper nanowires. *Nanotechnology*, 19, 21, (215712), 0957-4484

Gogotsi, Y., (2006). *Nanomaterials Handbook*, CRC, Taylor & Francis group, 0849323088, Florida.

Greenwood, J.A., Williamson, J.B.P., (1966). Contact of Nominally Flat Surfaces. *Proceedings of the Royal Society of London. Series A. Mathematical and Physical Sciences*, 295, 1442, (300-&), 0080–4630

Grujicic, M., Zhao, C.L., Dusel, E.C., (2005). The effect of thermal contact resistance on heat management in the electronic packaging. *Applied Surface Science*, 246, 1-3, (290), 0169-4332

Heather, D., Timothy, H., Elizabeth, M., Amit, G., Diana-Andra, B.-T., (2009). Fabrication of polydimethylsiloxane composites with nickel nanoparticle and nanowire fillers and study of their mechanical and magnetic properties. *Journal of Applied Physics*, 106, 6, (064909), 0021-8979

Huang, H., Liu, C.H., Wu, Y., Fan, S.S., (2005). Aligned carbon nanotube composite films for thermal management. *Advanced Materials*, 17, 13, (1652-1656), 0935-9648

Huang, Q., Lilley, C.M., Bode, M., (2009). Surface scattering effect on the electrical resistivity of single crystalline silver nanowires self-assembled on vicinal Si (001). *Applied Physics Letters*, 95, 10, (103112-103113), 0003-6951

ITRS, 2007. http://www.itrs.net/Links/2007ITRS/2007_Chapters/2007_Assembly.pdf.

Kalapi, G.B., Timothy, D.S., Baratunde, A.C., Xianfan, X., (2009). Thermal conductivity of bismuth telluride nanowire array-epoxy composite. *Applied Physics Letters*, 94, 22, (223116), 0003-6951

Kazeminezhad, I., Barnes, A.C., Holbrey, J.D., Seddon, K.R., Schwarzacher, W., (2007). Templated electrodeposition of silver nanowires in a nanoporous polycarbonate membrane from a nonaqueous ionic liquid electrolyte. *Applied Physics A: Materials Science & Processing*, 86, 3, (373-375), 0947-8396

Kempers, R., Frizzell, R., Lyons, A., A., R. (2009a). Development of a metal micro-textured thermal interface material. *Proceedings of the ASME 2009 InterPACK Conference, IPACK2009*, pp. San Francisco, CA, USA

Kempers, R., Robinson, A., Lyons, A. (2009b). Characterization of metal micro-textured thermal interface materials. *Thermal Investigations of ICs and Systems, 2009. THERMINIC 2009. 15th International Workshop on*, pp. 210-215, 978-1-4244-5881-3, Leuven

Lasance, C.J.M., Murray, C.T., Saums, D.L., Renez, M. (2006). Challenges in thermal interface material testing. *Semiconductor Thermal Measurement and Management Symposium, 2006 IEEE Twenty-Second Annual IEEE*, pp. 42-49, 1-4244-0153-4, Dallas, Texas

Liu, J., Michel, B., Rencz, M., Tantolin, C., Sarno, C., Miessner, R., Schuett, K.V., Tang, X., Demoustier, S., Ziaei, A. (2008a). Recent progress of thermal interface material research - an overview. *Thermal Inveatigation of ICs and Systems, 2008. THERMINIC 2008. 14th International Workshop on*, pp. 156-162, 978-1-4244-3365-0, Rome

Liu, J., Teng, W., Carlberg, B., Inoue, M. (2008b). Recent progress of thermal interface materials. *Electronics System-Integration Technology Conference, 2008. ESTC 2008. 2nd*, pp. 351-358, 978-1-4244-2813-7, Greenwich

Lonjon, A., Laffont, L., Demont, P., Dantras, E., Lacabanne, C., (2009). New Highly Conductive Nickel Nanowire-Filled P(VDF-TrFE) Copolymer Nanocomposites: Elaboration and Structural Study. *The Journal of Physical Chemistry C*, 113, 28, (12002-12006), 1932-7447

Mahajan, R. (2002). Thermal management of CPUs: A perspective on trends, needs and opportunities. *Invited talk given at the Eighth International Workshop on Thermal Investigations of ICs and Systems (THERMINIC)*, pp. October 1-4, Madrid, Spain

Melechko, A.V., Merkulov, V.I., McKnight, T.E., Guillorn, M.A., Klein, K.L., Lowndes, D.H., Simpson, M.L., (2005). Vertically aligned carbon nanofibers and related structures: Controlled synthesis and directed assembly. *Journal of Applied Physics*, 97, 4, (39), 0021-8979

Munari, A., Ju, X., Dalton, E., Mathewson, A., Razeeb, K.M. (2009). Metal nanowire-polymer nanocomposite as thermal interface material. *59th Electronic Components and Technology Conference, 2009. ECTC 2009*, pp. 448-452, 0569-5503, ECTC, San Diego

Nan, C.W., Shi, Z., Lin, Y., (2003). A simple model for thermal conductivity of carbon nanotube-based composites. *Chemical Physics Letters*, 375, 5-6, (666-669), 0009-2614

Ngo, Q., Cruden, B.A., Cassell, A.M., Sims, G., Meyyappan, M., Li, J., Yang, C.Y., (2004). Thermal Interface Properties of Cu-filled Vertically Aligned Carbon Nanofiber Arrays. *Nano Letters*, 4, 12, (2403-2407), 1530-6984

Panzer, M.A., Zhang, G., Mann, D., Hu, X., Pop, E., Dai, H., Goodson, K.E., (2008). *Journal of Heat Transfer-Transactions of the ASME*, 130, (052401),

Parker, W.J., Jenkins, R., Butler, C.P., Abbot, G.L., (1961). *Journal of Applied Physics*, 32, 9, (1679), 0021-8979

Prasher, R., (2006). Thermal interface materials: Historical perspective, status, and future directions. *Proceedings of the IEEE*, 94, 8, (1571), 0018-9219

Prasher, R.S., (2001). Surface chemistry and characteristics based model for the thermal contact resistance of fluidic interstitial thermal interface materials. *Journal of Heat Transfer-Transactions of the ASME*, 123, 5, (969), 0022-1481

Prasher, R.S., Koning, P., Shipley, J., Devpura, A., (2003). Dependence of thermal conductivity and mechanical rigidity of particle-laden polymeric thermal interface material on particle volume fraction. *Journal of Electronic Packaging*, 125, 3, (386), 1043-7398

Razeeb, K.M., Munari, A., Dalton, E., Punch, J., Roy, S. (2007). Thermal Properties of Carbon Nanotube-Polymer Composites for Thermal Interface Material. *2007 ASME-JSME Thermal Engineering Conference and Summer Heat Transfer Conference* pp. 817-823, 0-7918-4275-4, ASME, Vancouver, BC

Razeeb, K.M., Roy, S., (2008). Thermal diffusivity of nonfractal and fractal nickel nanowires. *Journal of Applied Physics*, 103, 8, (084302), 0021-8979

Rodgers, P., Eveloy, V., Pecht, M.G. (2005). Extending the limits of air-cooling in microelectronic equipment. *Thermal, Mechanical and Multi-Physics Simulation and Experiments in Micro-Electronics and Micro-Systems, 2005. EuroSimE 2005. Proceedings of the 6th International Conference on*, pp. 695-702, 0-7803-9062-8, Berlin, Germany

Sauciuc, I., Prasher, R., Chang, J.-Y., Erturk, H., Chrysler, G., Chiu, C.-P., Mahajan, R. (2005). Thermal Performance and Key Challenges for Future CPU Cooling Technologies. *ASME Conference Proceedings*, pp. 353-364, 0-7918-4200-2, San Francisco, California, USA

Savija, I., Culham, J.R., Yovanovich, M.M., Marotta, E.E., (2003). Review of thermal conductance models for joints incorporating enhancement materials. *Journal of Thermophysics and Heat Transfer*, 17, 1, (43-52), 0887-8722

Schelling, P.K., Shi, L., Goodson, K.E., (2005). Managing heat for electronics. *Materials Today*, 8, 6, (30-35), 1369-7021

Singhal, V., Siegmund, T., Garimella, S.V., (2004). Optimization of thermal interface materials for electronics cooling applications. *IEEE Transactions on Components and Packaging Technologies*, 27, 2, (244-252), 1521-3331

Sondheimer, E.H., (1952). The mean free path of electrons in metals. *Advances in Physics*, 1, 1, (1 - 42), 0001-8732

Srivastava, D., Wei, C., Cho, K., (2003). Nanomechanics of carbon nanotubes and composites. *Applied Mechanics Reviews*, 56, 2, (215-230), 0003-6900

Steinhögl, W., Schindler, G., Steinlesberger, G., Engelhardt, M., (2002). Size-dependent resistivity of metallic wires in the mesoscopic range. *Physical Review B*, 66, 7, (075414), 1098-0121

Sun, L., Keshoju, K., (2008). Polymer Composites with Oriented Magnetic Nanowires as Fillers. *Mater. Res. Soc. Symp. Proc.*, 1058, (JJ06-26), 0272-9172

Torresola, J., Chiu, C.P., Chrysler, G., Grannes, D., Mahajan, R., Prasher, R., Watwe, A., (2005). Density factor approach to representing impact of die power maps on thermal management. *Ieee Transactions on Advanced Packaging*, 28, 4, (659), 1521-3323

Viswanath, R., Wakharkar, V., Watwe, A., Lebonheur, V., (2000). Thermal Performance Challenges from Silicon to Systems. *Intel Technology Journal*, 4, 3, (16), 1535-864X

Weast, R.C., (1994). *CRC Handbook of Chemistry and Physics*, CRC Press, 0849305667, Florida.

White, S.I., Mutiso, R.M., Vora, P.M., Jahnke, D., Hsu, S., Kikkawa, J.M., Li, J., Fischer, J.E., Winey, K.I., (2010). Electrical Percolation Behavior in Silver Nanowire–Polystyrene Composites: Simulation and Experiment. *Advanced Functional Materials*, 20, 16, (2709-2716), 1616-3028

Wu, Y., Liu, C.H., Huang, H., Fan, S.S., (2005). Effects of surface metal layer on the thermal contact resistance of carbon nanotube arrays. *Applied Physics Letters*, 87, 21, (213108), 0003-6951

Wunderle, B.K., M. Dietrich, L. Abo Ras, M. Mrossko, R. May, D. Schacht, R. Oppermann, H. and Michel, B. (2010). Advances in thermal interface technology: mono-metal

interconnect formation, processing and characterisation (Submitted). *Proceedings of the iTherm 2010 Conference*, pp. 1 - 10, 978-1-4244-5342-9, Las Vegas, NV, USA

Xu, G., 2006. Thermal management for electronic packaging. *Lecture on Heat Dissipation*. University of California, San Diego, CA, USA.

Xu, J., Fisher, T.S., (2006). Enhancement of thermal interface materials with carbon nanotube arrays. *International Journal of Heat and Mass Transfer*, 49, 9-10, (1658-1666), 0017-9310

Xu, J., Razeeb, K.M., Roy, S., (2008). Thermal properties of single walled carbon nanotube-silicone nanocomposites. *Journal of Polymer Science Part B: Polymer Physics*, 46, 17, (1845-1852), 1099-0488

Xu, J., Munari, A., Dalton, E., Mathewson, A., Razeeb, K.M., (2009). Silver nanowire array-polymer composite as thermal interface material. *Journal of Applied Physics*, 106, 12, (124310), 0021-8979

Zeng, J., Cao, Z., Yang, D., Sun, L., Zhang, L., (2009). Thermal conductivity enhancement of Ag nanowires on an organic phase change material. *Journal of Thermal Analysis and Calorimetry*, 101, 1, (385-389), 1388-6150

Zhang, W., Brongersma, S.H., Richard, O., Brijs, B., Palmans, R., Froyen, L., Maex, K., (2004). Influence of the electron mean free path on the resistivity of thin metal films. *Microelectronic Engineering*, 76, 1-4, (146-152), 0167-9317